View metadata, citation and similar papers at core.ac.uk
brought to you by CORE
provided by RERO DOC Digital Library

Mon. Not. R. Astron. Soc. **380,** 691–702 (2007) doi:10.1111/j.1365-2966.2007.12160.x

Millisecond pulsars around intermediate-mass black holes in globular clusters

B. Devecchi,[1⋆] M. Colpi,[1] M. Mapelli[2] and A. Possenti[3]

[1]*Dipartimento di Fisica G. Occhialini, Università degli Studi di Milano Bicocca, Piazza della Scienza 3, I-20126 Milano, Italy*
[2]*Institute for Theoretical Physics, University of Zürich, Winterthurerstrasse 190, CH-8057 Zürich, Switzerland*
[3]*INAF, Osservatorio Astronomico di Cagliari, Poggio dei Pini, Strada 54, I-09012 Capoterra, Italy*

Accepted 2007 May 11. Received 2007 May 7; in original form 2006 December 29

ABSTRACT

Globular clusters (GCs) are expected to be breeding grounds for the formation of single or binary intermediate-mass black holes (IMBHs) of $\gtrsim 100\,M_\odot$, but a clear signature of their existence is still missing. In this context, we study the process of dynamical capture of a millisecond pulsar (MSP) by a single or binary IMBH, simulating various types of single–binary and binary–binary encounters. It is found that [IMBH, MSP] binaries form over cosmic time in a cluster, at rates $\lesssim 10^{-11}$ yr^{-1}, via encounters of wide-orbit binary MSPs off the single IMBH, and at a lower pace, via interactions of (binary or single) MSPs with the IMBH orbited by a typical cluster star. The formation of an [IMBH, MSP] system is strongly inhibited if the IMBH is orbited by a stellar mass black hole (BH): in this case, the only viable path is through the formation of a rare stable hierarchical triplet with the MSP orbiting exterior to the [IMBH, BH] binary. The [IMBH, MSP] binaries that form are relatively short-lived, $\lesssim 10^8 - 10^9$ yr, since their orbits decay via emission of gravitational waves. The detection of an [IMBH, MSP] system has a low probability of occurrence, when inferred from the current sample of MSPs in GCs. If next-generation radio telescopes, like Square Kilometre Array (SKA), will detect an order of magnitude larger population of MSP in GCs, at least one [IMBH, MSP] is expected. Therefore, a complete search for low-luminosity MSPs in the GCs of the Milky Way with SKA will have the potential of testing the hypothesis that IMBHs of the order of $100\,M_\odot$ are commonly hosted in GCs. The discovery will unambiguously prove that BHs exist in the still uncharted interval of masses around $\gtrsim 100\,M_\odot$.

Key words: black hole physics – stellar dynamics – stars: neutron – pulsars: general – globular clusters: general.

1 INTRODUCTION

1.1 IMBHs: observations

A number of observations suggest that intermediate-mass black holes (IMBHs) may exist with masses between $\approx 100\,M_\odot$ to $10^4\,M_\odot$. Heavier than the stellar mass black holes (BHs) born in core-collapse supernovae (3–30 $M_\odot$; Orosz 2003), IMBHs are expected to form in dense, rich stellar systems through complex dynamical processes. Globular clusters (GCs), among the densest stellar systems known in galaxies, have therefore become prime sites for their search.

Gebhardt, Rich & Ho (2002, 2005) suggested the presence of an IMBH of $2^{+1.4}_{-0.8} \times 10^4\,M_\odot$, in the cluster G1 of M31, on the basis of a joint analysis of photometric and spectroscopic measurements. Remarkably, the IMBH in G1 seems to lie just on the low end of the BH mass versus one-dimensional dispersion velocity correlation observed in spheroids and bulges of nearby galaxies (Ferrarese & Merritt 2000; Gebhardt et al. 2000).

In the Galactic GC M15, *Hubble Space Telescope* and ground-based observations of line-of-sight velocities and proper motions, indicated the occurrence of a central concentration of non-luminous matter of $500^{+2500}_{-500}\,M_\odot$, that could be ascribed to the presence of an IMBH (Gerssen et al. 2002; van den Bosch et al. 2006). By mapping the velocity field, van den Bosch et al. (2006) found also evidence of ordered rotation in the central 4 arcsec of M15. This unexpected dynamical state in a region of rapid relaxation (10^7 yr) may give first evidence, albeit indirect, that a source of angular momentum in the form of a 'binary' IMBH may exist in M15 (Mapelli et al. 2005). Claims of the possible presence of an IMBH have been advanced also in 47 Tucanae (McLaughlin et al. 2006).

⋆E-mail: bernadetta.devecchi@mib.infn.it

© 2007 The Authors. Journal compilation © 2007 RAS

An additional puzzling picture has emerged from observations in NGC 6752. Two millisecond pulsars (MSPs hereon), PSR-B and PSR-E, show unusual accelerations (D'Amico et al. 2002), that, once ascribed to the overall effect of the cluster potential well, indicate the presence of $\gtrsim 1000\,M_\odot$ of underluminous matter enclosed within the central 0.08 pc (Ferraro et al. 2003a). NGC 6752 is even more peculiar than M15, since it also hosts two MSPs with unusual locations. PSR-A, a binary pulsar with a white dwarf (WD) companion (D'Amico et al. 2002; Bassa et al. 2003; Ferraro et al. 2003b) and a very low orbital eccentricity($\sim 10^{-5}$, D'Amico et al. 2002) holds the record of being the farthest MSP ever observed in a GC, at a distance of $\approx$3.3 half-mass radii. PSR-C, an isolated MSP, ranks second in the list of the most offset pulsars known, at a distance of 1.4 half-mass radii from the gravitational centre of the cluster (D'Amico et al. 2002; Corongiu et al. 2006). Colpi, Possenti & Gualandris (2002) first conjectured that PSR-A was propelled into the halo in a fly-by off a binary BH in the mass range between 10 and $100\,M_\odot$ opening the perspective of unveiling binary BHs in GCs (see Section 1.2). Prompted by the evidence of underluminous matter in the core of NGC 6752, Colpi, Mapelli & Possenti (2003) carried on an extensive analysis of binary–binary encounters with IMBHs, to asses the viability of this scenario. They found that a $\sim 100\,M_\odot$ IMBH with a stellar mass BH in a binary would be the best target for imprinting the necessary thrust to PSR-A[1] and at the same time for preserving the low eccentricity of the binary pulsar (within a factor of 3 for the bulk of the simulated encounters). Instead, larger mass IMBHs ($\sim 500\,M_\odot$) with star companions can produce the correct ejection velocity, but cause the eccentricity to grow much larger. Thus, PSR-A had to interact with the very massive IMBH only before its recycling phase.

The observation of IMBHs in GCs is still far from being conclusive, since numerical studies have shown that kinematic features as those observed in G1 and M15 can be reproduced assuming, in the cluster centre, the presence of a collection of low-mass compact remnants, with no need of a single massive IMBH (Baumgardt et al. 2003a,b). In addition, a single massive ($\gtrsim 1000\,M_\odot$) IMBH, if present, would affect the stellar dynamics (because of energy generation in the IMBH cusp) creating a constant density profile of bright stars in projection that differs from the typical profile of a core-collapse cluster such as M15 (Baumgardt, Makino & Ebisuzaki 2004).

1.2 IMBHs: theory

On theoretical ground a number of authors suggested that IMBHs may form inside either (i) young and dense star clusters vulnerable to unstable mass segregation and core-collapse before the most massive stars explode as supernovae (Portegies Zwart & McMillan 2002; Freitag, Gürkan & Rasio 2006; Gürkan, Fregeau & Rasio 2006) or (ii) dynamically in already evolved GCs when all the massive stars have turned into stellar mass BHs (Miller & Hamilton 2002). In the first case, runaway collisions among young massive stars may lead to the formation of a very massive stellar object which ultimately collapses into an IMBH.[2] In the second case, IMBH formation requires a succession of close gravitational encounters among stellar mass BHs: being the heaviest objects in the cluster, these BHs may segregate in the core under the action of the Spitzer's mass stratification instability (Spitzer 1969; Lightman & Fall 1978; Watters, Joshi & Rasio 2000; Khalisi, Amaro-Seoane & Spurzem 2007), forming a dense core which becomes dynamically decoupled from the rest of the stars. Hardening and recoil among the interacting BHs lead to their ejection from the cluster (Kulkarni, Hut & McMillan 1993; Sigurdsson & Hernquist 1993; Portegies Zwart & McMillan 2000) and at the same time to the increase of their mass because of repeated mergers (Miller & Hamilton 2002). O'Leary et al. (2006) have recently shown that there is a significant probability (between 20 and 80 per cent) of BH growth, and found final masses $\gtrsim 100\,M_\odot$. After evaporation of most of the BHs on a time-scale of $\sim$ Gyr, one IMBH and/or few BHs, single or in binaries, may remain inside the GC.

The recent discovery of a luminous, highly variable X-ray source in one GC of NGC 4472 (Maccarone et al. 2007) may have just provided first evidence that at least one BH is retained inside. Whether this source in NGC 4472 is an accreting BH or IMBH is still uncertain, but this finding goes in the direction noted by Pfahl (2005), who considered the possibility that an IMBH would tidally capture a star leading to the turn-on of a bright X-ray source.

Given all these uncertainties and the importance of establishing the possible existence of IMBH in GCs, we explore in this paper an alternative root, that is, the possibility that gravitational encounters off the IMBH provide a path for the dynamical capture of an MSP and the formation of a binary (hereafter labelled [IMBH, MSP]) comprising the IMBH and the MSP. Timing of the radio signal emitted by the MSP would provide in this way a direct, unambiguous measure of the BH mass.

Motivated by the observation of the halo MSPs in NGC 6752, we simulate a series of dynamical interactions between a binary MSP and a single or a binary IMBH, and also between a single MSP and a binary IMBH. In the context adopted, the binary IMBH may have a stellar mass BH, or a star, as companion.

The outline of the paper is as follows. In Section 2, we describe the initial conditions of the three- and four-body encounters. In Section 3, we compute cross-sections for the formation of [IMBH, MSP] systems coming from encounters with PSR-A like MSP binaries. We study the orbital characteristics of the [IMBH, MSP] binaries in their end states, and explore the stability of triple systems that form, against dynamical and resonant self-interactions. Binary systems composed by the WD and the IMBH are also considered, and the results are shortly summarized in Section 4. In Section 5, we show the results obtained from simulations with binary MSPs different from PSR-A that represent the observed population in GCs. We study their end states and their characteristic lifetimes taking into account for their hardening by cluster stars and by gravitational wave driven in-spiral. In Section 6 we study the detectability of MSPs around IMBHs in GCs and discuss the potential importance of these systems for next-generation deep radio surveys in the Galactic halo. In Section 7 we summarize our findings.

[1] Ejection of PSR-A from the core to the halo following exchange interactions off normal binary stars cannot be excluded, but as pointed out by Colpi et al. (2002); Sigurdsson (2003), the binary parameters of PSR-A and its evolution make this possibility remote, and call for fine tuning conditions.

[2] The effects of the environment, of rotation and metallicity, on the formation and fate of these ultramassive stars are largely unknown. A recent study on the mass loss of merged stars (during and after the merger) of $\sim 100\,M_\odot$ have shown that this does not seem to inhibit the formation of very massive stars (Suzuki et al. 2007). However, further studies are needed in order to better constrain the evolution of those more massive object ($\sim 1000\,M_\odot$) that should form $\sim 1000\,M_\odot$ IMBH.

2 GRAVITATIONAL ENCOUNTERS

2.1 The projectile

We consider encounters in which the projectile is either a [MSP, WD] binary, or a single MSP. As first case study, we simulate [MSP, WD] systems similar to PSR-A in NGC 6752: the MSP has a mass $m_{\rm MSP} = 1.4\,{\rm M}_\odot$ and a WD companion of $m_{\rm WD} = 0.2\,{\rm M}_\odot$; the binary has semimajor axis $a_{\rm MSP,i} = 0.0223$ au, orbital period of 0.86 d, and orbital eccentricity $e_{\rm MSP,i} = 10^{-5}$.

We then simulate binary MSPs whose characteristics are extrapolated from the observed sample of MSPs belonging to the GCs of the Milky Way (Camilo & Rasio 2005) (see Section 5 for further discussion). For the single MSP, we consider $m_{\rm MSP} = 1.4\,{\rm M}_\odot$.

2.2 The target IMBH

The target is an IMBH, either single or binary, and has no stellar cusp (Baumgardt et al. 2004). In agreement with O'Leary et al. (2006) and Colpi et al. (2003), its mass $M_{\rm IMBH}$ is either 100 or $300\,{\rm M}_\odot$.

The binary IMBHs have initial semimajor axes and eccentricities drawn from probability distributions that account for their physical conditions in a GC. In details, the initial properties of the target [IMBH, star] and [IMBH, BH] binaries are the following.

(i) IMBH, star: We randomly generate the mass m_* of the star, the semimajor axis a_* and the eccentricity e_*. The values for m_* follow a current mass function biased towards massive stars, in order to account for dynamical mass segregation in the core of the cluster. We thus consider a mass function ${\rm d}N/{\rm d}m \propto m^{-(1+x)}$ with $x = -5$ as inferred from observations of 47 Tucanae (Monkman et al. 2006) with an upper cut-off mass of $0.95\,{\rm M}_\odot$. For the semimajor axes we follow the analysis proposed by Pfahl (2005) and briefly summarized in Appendix A. The values of a_* refer to conditions acquired in dynamical ionization of incoming stellar binaries off an initially single IMBH. Table 1 gives the initial minimum and maximum semimajor axes used at the onset of the simulations. The eccentricity e_* follows a thermal distribution (Blecha et al. 2006). The same distribution for a_*, e_* and m_* is used for the interaction of the [IMBH, star] binary both with [MSP, WD] and single MSP. To distinguish these two cases, hereon we will refer to the latter using the subscript 'MSP, single'.

(ii) IMBH, BH: The IMBH has a BH companion of $m_{\rm BH} = 10\,{\rm M}_\odot$. The binary has semimajor axis $a_{\rm BH}$ drawn from two distinct probability distributions, which have been derived:

(1) from the hardening due to encounters off cluster stars (subscript [h, $*$], hereon), occurring on a time-scale (Quinlan 1996; Mapelli et al. 2005)

$$t_{\rm h}(a) \sim \frac{\langle v_*\rangle}{(2\pi\xi)\,G\langle\rho_*\rangle}\frac{1}{a_{\rm BH}} = 2\times10^7 v_{10} a_5^{-1}\rho_{5.8}^{-1}\ {\rm yr}, \quad (1)$$

where $\langle\rho_*\rangle$, $\langle v_*\rangle$ and ξ are the mean stellar mass density, dispersion velocity and hardening efficiency [we assume $\langle v_*\rangle = 10\,v_{10}\,{\rm km\,s^{-1}}$, $\xi = 1$ (Colpi et al. 2003), $a_{\rm BH} = 5\,a_5$ au and for the density $\langle\rho_*\rangle = 7\times10^5\,\rho_{5.8}\,{\rm M}_\odot\,{\rm pc}^{-3}$, the value inferred averaging over the GC sample currently hosting the population of known MSPs (see Section 5)];

(2) from the in-spiral driven by gravitational wave back-reaction (subscript gw, hereon), when the binary is tight (see Section A1 for details). The corresponding time-scale, function of the semimajor axis $a_{\rm BH}$ and eccentricity $e_{\rm BH}$ (Peters & Mathews 1963) is

$$t_{\rm gw}(a_{\rm BH}, e_{\rm BH}) \equiv \frac{5}{256}\frac{c^5 a_{\rm BH}^4\left(1-e_{\rm BH}^2\right)^{7/2}}{G^3 m_{\rm BH} M_{\rm IMBH}\,(m_{\rm BH}+M_{\rm IMBH})} = 4.4\times10^8 a_{0.2}^4 M_{100}^{-1} m_{10}^{-1} M_{\rm T,110}^{-1}\ {\rm yr}, \quad (2)$$

where the following normalizations are used to estimate $t_{\rm gw}$ for $e_{\rm BH} = 0.7$: $a_{\rm BH} = 0.2\ a_{0.2}$ au, $M_{\rm IMBH} = 100\ M_{100}\,{\rm M}_\odot$, $m_{\rm BH} = 10\ m_{10}\,{\rm M}_\odot$ and $M_{\rm T} = M_{\rm IMBH} + m_{\rm BH} = 110\ M_{\rm T,110}\,{\rm M}_\odot$. The peak of the composite semimajor axis distribution occurs when the two processes become comparable, that is, at a distance

$$a_{\rm gw}(e_{\rm BH}) \sim \left[\frac{256}{5}\frac{G^2 m_{\rm BH} M_{\rm IMBH}\,(m_{\rm BH}+M_{\rm IMBH})\,\langle v_*\rangle}{\left(1-e_{\rm BH}^2\right)^{7/2} c^5\langle\rho_*\rangle\,2\pi\xi}\right]^{1/5} \quad (3)$$

corresponding to $t_{\rm h} = t_{\rm gw}$, inferred from equations (1) and (2). Typical separations for our [IMBH, BH] binaries are $\sim$0.3 au.

In the hardening phase by stars the eccentricity $e_{\rm BH}$ is extracted from a thermal distribution, while during the gravitational wave driven phase the values of $e_{\rm BH}$ are inferred considering the modifications induced by gravitational wave loss (see Section A1).

Table 1. Initial parameters for simulations with PSR-A like initial MSP binaries. Rows refer to different initial states of the IMBH (referred as channels in the text). The different columns refer to: selected IMBH mass, minimum and maximum values for the distribution of the semimajor axis (for the [IMBH, star] and [IMBH, BH] binaries) and number of runs for each simulation. The first eight lines refer to encounters with the [MSP, WD] binary, the last two refer to encounters with a single MSP.

M ($\rm M_\odot$)	$a_{\rm m}$ (au)	$a_{\rm m}$ (au)	N
100	–	–	5000
300	–	–	5000
[100, star]	0.2	200	3000
[300, star]	0.42	417	3000
$[100, 10]_{\rm h,*}$	0.24	1960	5000
$[300, 10]_{\rm h,*}$	0.4	5526	5000
$[100, 10]_{\rm gw}$	2.2×10^{-3}	0.24	10 000
$[300, 10]_{\rm gw}$	3.2×10^{-3}	0.4	10 000
$[100, {\rm star}]_{\rm MSP,single}$	0.2	200	5000
$[300, {\rm star}]_{\rm MSP,single}$	0.42	417	5000

2.3 Code and outcomes

We run the numerical code CHAIN (kindly suited by S. Aarseth) which makes use of a Bulirsch–Stoer variable step integrator with KS-chain regularization. The code FEBO (FEw-BOdy), based on a fifth-order Runge–Kutta scheme (described in Colpi et al. 2003 and Mapelli et al. 2005), has been used for trial runs and gives results in nice agreement with CHAIN.

The impact parameters of the incoming binaries are distributed uniformly in b^2 (Hut & Bahcall 1983) up to a maximum value $b_{\rm max}^2$ (see Section A3). The phases of the binaries and the angles describing the initial direction and inclination of the encounter are extracted from the distributions by Hut & Bahcall (1983). The relative speed v_∞ has been sampled at random from a uniform distribution, in the range 8–12 $\rm km\,s^{-1}$, consistent with the values of NGC 6752 (Dubath, Meylan & Mayor 1997). The relative distance between the centres of mass of the interacting binaries is set equal to the gravitational influence radius of the target IMBH, $r_{\rm inf} \sim 2GM_{\rm IMBH}/\langle v_\infty\rangle^2$

© 2007 The Authors. Journal compilation © 2007 RAS, MNRAS **380,** 691–702

Table 2. Occurrence fractions ($f_{\rm MSP}$ and $f_{\rm WD}$) and cross-sections ($\Sigma_{\rm MSP}$ and $\Sigma_{\rm WD}$) calculated from equation (5) of [IMBH, MSP] and [IMBH, WD] binaries for each initial state of the IMBH, and for PSR-A like MSP binaries. Bracket (tr, in) denotes the occurrence of stable triplets where the MSP or the WD binds, forming the inner binary. Bracket (tr, ou) denotes the occurrence of stable triplets where the MSP or WD binds, forming the outer binary. The last two lines correspond to exchanges of a single MSP off the [IMBH, star] binary.

M ($\rm M_\odot$)	$f_{\rm MSP}$ (per cent)	$f_{\rm WD}$ (per cent)	$\Sigma_{\rm MSP}$ (au^2)	$\Sigma_{\rm WD}$ (au^2)
[100]	7.1	5.6	223	176
[300]	11.2	10	350	315
[100, star]	3	0.63(tr,in)	440	92
[300, star]	0.8	0.15(tr, in)	157	28
$[100, 10]_{\rm h,*}$	0.06(tr, in)	0.46(tr, in)	3.6	27
$[300, 10]_{\rm h,*}$	–	0.16(tr, in)	–	19
$[100, 10]_{\rm gw}$	0.19(tr, ou)	0.04(tr, ou)	2.4	0.5
$[300, 10]_{\rm gw}$	0.26(tr, ou)	0.04(tr, ou)	36	5.5
$[100, {\rm star}]_{\rm MSP,single}$	1.6	–	126	–
$[300, {\rm star}]_{\rm MSP,single}$	0.65	–	66	–

($\sim$2000 au for the 100 $\rm M_\odot$ case,[3] obtained for a stellar dispersion of 10 km s^{-1}).

After each single–binary encounter we can classify the end states as following:

(A) Fly-by: the binary maintains its components, but it can exit with a different energy and angular momentum.

(B) Tidal disruption: the interacting binary is broken by the massive IMBH. The tidal disruption can end with an ionization (B.1), if the final system consists of three single bodies, or with an exchange (B.2), if one of the two components is captured by the single. The tidal perturbation occurs at a distance $r_{\rm T} = a_{\rm MSP,i}\,[M_{\rm IMBH}/(m_{\rm MSP} + m_{\rm WD})]^{1/3}$, where the gradient exerted by the IMBH on the incoming binary exceeds its binding energy. For our binary pulsar, $r_{\rm T} \sim 0.1$ au.

In the case of binary–binary encounters the possible end states are analogous (i.e. fly-bies and tidal disruptions), but complicated by the fact that the interacting binaries are two. In particular, we can observe the tidal disruption of only one of the two binaries (mostly the softer [MSP, WD] binary), or of both of them. After the tidal disruption of the [MSP, WD] binary:

(B.1) The [MSP, WD] can be fully ionized (i.e. both components escape).

(B.2) One of the two components remains bound to the [IMBH, star] or [IMBH, BH] binary, forming a stable/unstable triplet. Some triplets show a characteristic configuration of two nested binaries, where two of the three components are bound in a tight binary, while the third one orbits around. This type of systems is termed hierarchical triplets.

A hierarchical triple is stable if it satisfies the relation (Mardling & Aarseth 1999)

$$\frac{R_{\rm p}}{a_{\rm in}} \geqslant 2.8 \left[(1+q)\,\frac{1+e_{\rm ou}}{\sqrt{1-e_{\rm ou}^2}} \right]^{2/5}, \qquad (4)$$

where $R_{\rm p}$ is the pericentre of the outer binary, $a_{\rm in}$ the semimajor axis of the inner binary, $e_{\rm ou}$ the eccentricity of the outer binary and q the mass ratio between the external component and the inner binary. If the triplet is unstable, the evolution of the system ends with the expulsion of one of the three components (preferentially, the less bound companion).

In the simulations, the integration is halted when the outgoing unbound star(s) is (are) at a sufficiently large distance from the centre of mass of the target binary or of the newly formed binary (or triplet). This maximum distance has been chosen equal to 50 times the semimajor axis of the system left. If the outgoing star (or binary) is still at such a distance after at least 2000 time-units, we stop the integration and we classify the encounter as an unresolved resonance.

[3] For the 300 $\rm M_\odot$ IMBH, the larger initial distance (6000 au) makes prohibitive the integration time for the simulations run with FEBO. For this reason integration starts at 2000 au after correcting for the relative parabolic motion. For consistency, we have chosen to adopt the same corrections also for the simulations run with CHAIN.

3 [IMBH, MSP] BINARIES

3.1 Cross-sections

We are interested in deriving the frequency of encounters ending with the formation of an [IMBH, MSP] binary. Thus, we computed $f_{\rm X} \equiv N_{\rm X}/N$, that is, the probability factor associated to channel X, where N is the total number of runs, and $N_{\rm X}$ is the number of cases in which event X occurs. The cross-section for channel X can be written as

$$\Sigma_{\rm X} = \pi f_{\rm X}\, b_{\rm max}^2, \qquad (5)$$

where $b_{\rm max}^2$ is the square of the maximum impact parameter that includes 'all' relevant encounters leading to X (Sigurdsson & Hernquist 1993; see Section A3 for its operative definition). Table 2 summarizes our results.

(i) In the encounters between the single IMBH and the [MSP, WD], we find that ionization of the incoming binary leads to the formation of [IMBH, MSP] systems with an occurrence $\sim$10 per cent. The cross-section in physical units is about a few hundreds au^2, and increases with the IMBH mass.

(ii) IMBH, star: In the case of binary–binary encounters with the target binary [IMBH, star], we often observe the exchange between the star and the heavier MSP, leading to the formation of an [IMBH, MSP] binary. The cross-section for the formation of the [IMBH, MSP] binary is slightly larger than for the isolated IMBH in the case of an IMBH of 100 $\rm M_\odot$, whereas the opposite holds for an IMBH of 100 $\rm M_\odot$.

(iii) [IMBH, star]$_{\rm MSP\ single}$: In the encounter of the [IMBH, star] and the single MSP we again observe the exchange of the star with the MSP, thus forming an [IMBH, MSP] system. We note that the frequency is a factor somewhat lower for the single MSP than in the [MSP, WD] case and this involves smaller cross-sections too.

(iv) IMBH, BH: In general, the presence of a massive companion such as a stellar mass BH does not favour the formation of an [IMBH, MSP], since the exchange probability is negligible. Triple systems may alternatively form. In rare cases ($\lesssim 0.1$ per cent) stable triplets can form with the MSP member of the inner binary [(IMBH, MSP), BH]. This occurs when the IMBH binary is in its hardening phase by dynamical encounters. When the [IMBH, BH] is in the phase of hardening by emission of gravitational waves, the MSP binds to the [IMBH, BH] as external companion with an higher probability ($f_{\rm X} \sim 0.2-0.3$ per cent) than in the hardening by scattering regime.

3.2 [IMBH, MSP] binary parameters

In this section we explore the properties of the [IMBH, MSP] systems that have formed dynamically. Fig. 1 shows the distribution of semimajor axes resulting from encounters with the $100\,{\rm M}_\odot$ IMBH. In the case of tidal disruption of the [MSP, WD] off the single IMBH, we find that the distribution peaks at $\sim$1 au. This value agrees with the analytical estimate (Pfahl 2005) obtained in the impulse approximation, that is, considering that the incoming [MSP, WD] binary is approaching the IMBH along a parabolic orbit, and that is disrupted instantaneously at the tidal radius $r_{\rm T}$. According to this analytical model (Pfahl 2005), the most likely end state has a binding energy per unit mass

$$E \sim -\frac{m_{\rm WD}}{m_{\rm MSP}+m_{\rm WD}} V_{\rm T} V_{\rm rel}, \tag{6}$$

where $V_{\rm T} \sim (GM_{\rm IMBH}/r_{\rm T})^{1/2}$ and $V_{\rm rel}$ is the relative velocity of the [MSP, WD] binary before the encounter. The corresponding

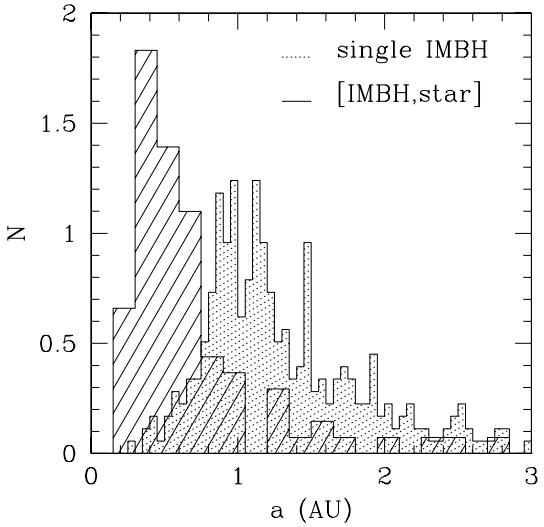

Figure 1. Distribution of the semimajor axes of the [IMBH, MSP] binaries, normalized to the corresponding fraction of events, for PSR-A like initial MSP binaries. The IMBH has a mass of $100\,{\rm M}_\odot$. Shaded histogram with dotted lines refers to [IMBH, MSP] systems formed after tidal disruption off the single IMBH. Shaded histogram with solid lines refers to the [IMBH, MSP] binaries that form after the exchange of the initial star in the [IMBH, star] binary.

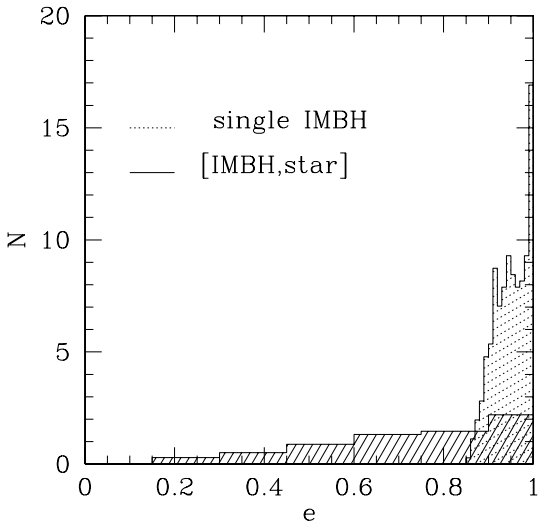

Figure 2. Distribution of eccentricities of [IMBH, MSP] binaries, normalized to the corresponding fraction of events. Shaded histograms refer to the same cases as in Fig. 1.

semimajor axis of the newly formed [IMBH, MSP] binary is

$$a_{\rm MSP,f} \sim \frac{a_{\rm MSP,i}}{2\sqrt{2}} \frac{M_{\rm IMBH}}{m_{\rm WD}} \left(\frac{m_{\rm MSP}+m_{\rm WD}}{M_{\rm IMBH}} \right)^{1/3} \tag{7}$$

which perfectly agrees with the results of our simulations ($a_{\rm MSP,f} \sim$ 1 au for a $100\,{\rm M}_\odot$ IMBH).

Fig. 1 also shows the distribution of the semimajor axes of the [IMBH, MSP] formed during the [MSP, WD] interaction off the [IMBH, star] binary, following the disruption of the [MSP, WD] at $\sim r_{\rm T}$ and the subsequent exchange of the MSP off the star. The MSP is captured on a close orbit, and, from simple energy arguments, the most likely end state is expected to have a specific energy

$$E \sim -\frac{m_{\rm WD}}{m_{\rm MSP}+m_{\rm WD}} V_{\rm T} V_{\rm rel} - \frac{m_*}{a_*} \frac{GM_{\rm IMBH}}{2m_{\rm MSP}}. \tag{8}$$

Indeed, during the triple encounter between the MSP, the star and the IMBH (after the expulsion of the WD), an energy (at least) equal to the binding energy of the star before ejection needs to be extracted, in order to unbind the star. The characteristic semimajor axis of the newly formed [IMBH, MSP] will thus be

$$a^*_{\rm MSP,f} \sim \frac{a_{\rm MSP,f}}{1+(m_*/m_{\rm MSP})\ a_{\rm MSP,f}/a_*}. \tag{9}$$

If we consider mean values for the initial m_*/a_* selecting all the systems that end with an [IMBH, MSP] binary, we find $m_*/a_* \sim 1.68\,{\rm M}_\odot/{\rm au}$. This corresponds to a semi-analytical estimate $a^*_{\rm MSP,f} \sim 0.45$ au, in good agreement with the peak of the corresponding semimajor axis distribution derived from our simulations (Fig. 1).

Fig. 2 shows the distribution of the eccentricities for the same binaries. For the case of tidal capture the eccentricities at which the MSP binds to the IMBH are above 0.9; for the formation channel through exchange the spread of the final eccentricity distribution is much larger, according to a thermal distribution. This can eventually be the effect of repeated interactions between the MSP and the initial companion of the IMBH during the transient state of unstable triplet. The distribution of the semimajor axis and eccentricity of [IMBH, MSP]$_{\rm MSP\ single}$ systems formed by the exchange off the single MSP are similar to the ones formed in the interaction of the [MSP, WD] off the [IMBH, star].

© 2007 The Authors. Journal compilation © 2007 RAS, MNRAS **380,** 691–702

Finally, we note that in the case of a 300 $M_\odot$ IMBH, the distributions are similar and only slightly skewed to larger values of the semimajor axes, as should be expected for a more massive BH (see equation 7).

3.3 Hierarchical triplets

As previously noted, the only way an MSP can be retained in the presence of an [IMBH, BH] binary is through the formation of hierarchical stable triple systems. Two possibilities exist: either the formation of an [(IMBH,MSP),BH] where the MSP is closely bound to the IMBH, or the formation of an [(IMBH,BH),MSP] with the MSP as external object.

Triple systems of the first type are rare, because the MSP tends to bind preferentially on orbits where its motion is gravitationally perturbed by the stellar mass BH causing the MSP to be finally ejected. Only triplets of the second type are seen to form with a non-negligible probability (∼0.2 per cent): the MSP binds on very wide (20–100 au), eccentric orbits (>0.6), as shown in Figs 3 and 4. The triplets in consideration are extremely hierarchical (i.e. $R_{\rm MSP,ou} \gg a_{\rm BH,in}$), in order to fulfil the stability condition.

Hierarchical triplets of this type are likely to survive inside the GC and to turn into an [IMBH, MSP]. Indeed, once the triplet has formed, the MSP shrinks its orbit with time due to dynamical encounters off cluster stars while the inner binary hardens due to gravitational wave emission. Since the hardening time of the inner binary is usually shorter than that of the outer binary, these triplets are transient states ending with the formation of a new [IMBH, MSP] binary following BH coalescence.

4 [IMBH, WD] BINARIES

For the sake of completeness, the results on the formation of [IMBH, WD] binaries are also summarized in Table 2. In the case of the capture of the WD by the single IMBH, we note that the occurrence fraction of [IMBH, WD] is only slightly lower than that of [IMBH, MSP] while it decreases by a factor of ∼5 for the [IMBH, star] cases, as shown in Table 2. If the IMBH has a companion star, the WD preferentially binds in triplet configurations. In fact the WD can be retained around the IMBH only if it forms a hierarchical triplet [(IMBH, WD), star]. This is due to the smaller mass of the WD relative to the star that makes exchanges very unlikely. The same is true for the [IMBH, BH] cases: stable triplets form with the WD in the inner binary, that is, [(IMBH, WD), BH], when the IMBH binary is hardening by scattering stars. On the contrary, the fraction of stable triplets significantly drops during the gravitational wave driven phase (∼0.04 per cent). This is due to the fact that the WD preferentially binds to the IMBH on an orbit strongly perturbed by the stellar mass BH. The cross-sections computed using equation (5) are reported in Table 2 and their values reflect their dependence upon $f_{\rm X}$.

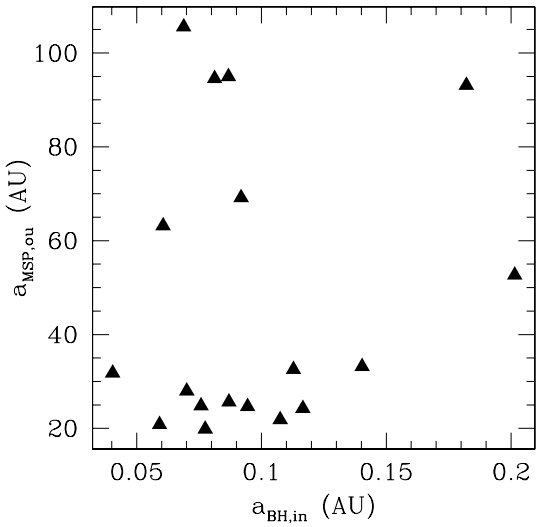

Figure 3. MSP semimajor axis $a_{\rm MSP,ou}$ of the outer binary versus semimajor axis $a_{\rm BH,in}$ of the inner binary [IMBH,BH] of stable hierarchical triple systems. The plot refers to an initial [IMBH, BH] binary of 100 and 10 $M_\odot$, and an initial PSR-A-like MSP binary.

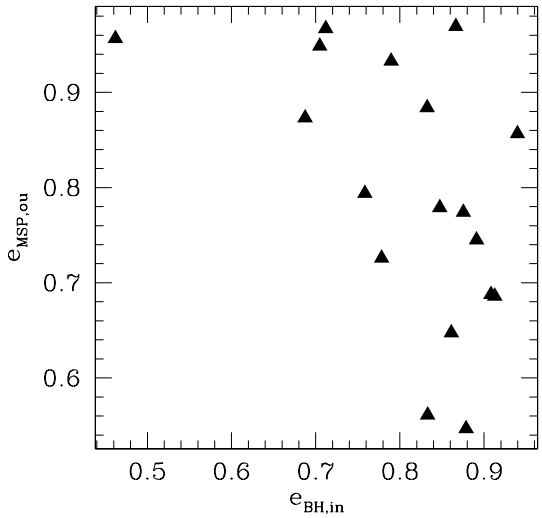

Figure 4. MSP eccentricity $e_{\rm MSP,ou}$ of the outer binary versus eccentricity $e_{\rm BH,in}$ of the inner binary (IMBH,BH) of stable hierarchical triple systems: the initial parameters of the involved binaries are the same as in Fig. 3.

Fig. 5 shows the distributions of the semimajor axis and eccentricity for the WD case, considering only the interaction with the single IMBH. Because of its lighter mass with respect to the MSP, the WD binds around the single IMBH on tighter orbits and the peak is around 0.17 au, in agreement with Pfahl's analysis (2005).[4]

The channel that we have outlined for the formation of an [IMBH, WD] binary is probably not the dominant one, because of the higher number of [WD, star] with respect to [MSP, WD] binaries. For this reason we have chosen not to discuss the formation rate of [IMBH, WD] binaries in more details.

5 [IMBH, MSP] IN GLOBULAR CLUSTERS

So far, we have considered only binary MSPs which mimic the properties of PSR-A in NGC 6752. Compared to PSR-A however, binary MSPs in GCs display a wider distribution of properties in their orbits and masses (Harris 1996; Camilo & Rasio 2005). Since the cross-section for the formation of [IMBH, MSP] systems as well as their ending states depend on the initial semimajor axes and total mass of the impinging [MSP, WD] binaries, in this section we have simulated a set of interactions varying the properties of the binary MSP.

[4] If the WD is captured instead of the MSP, equation (7) is modified to take into account for the different mass of the expelled star, thus giving $a_{\rm WD,f} \sim \frac{a_{\rm MSP,i}}{2\sqrt{2}} \frac{M_{\rm IMBH}}{m_{\rm MSP}} \left(\frac{m_{\rm MSP}+m_{\rm WD}}{M_{\rm IMBH}}\right)^{1/3} = 0.14 M_{100}^{2/3}$ au.

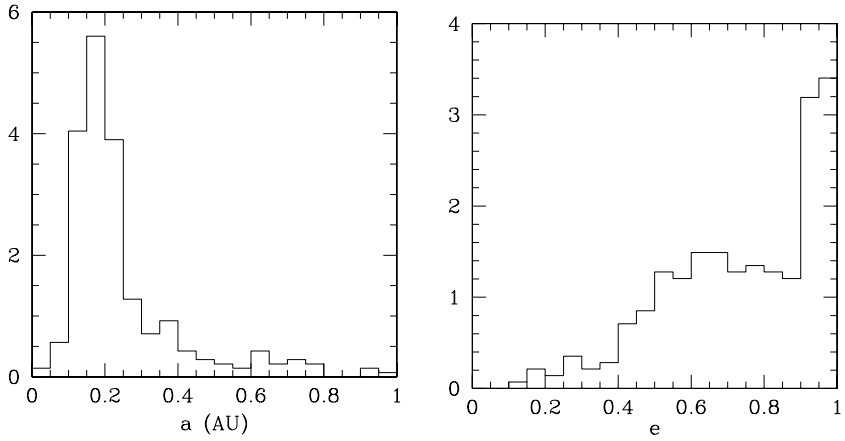

Figure 5. Distributions of semimajor axis and eccentricities of the [IMBH, WD] binaries, normalized to the corresponding fraction of events, for the single IMBH of 100 $M_\odot$, and a PSR-A like initial MSP binary.

Binary MSPs in GCs show a double peaked distribution of their semimajor axes in the interval [0.0024, 0.035 au], while a number of 'outliers' spread over larger orbital separations (see fig. 3 in Camilo & Rasio 2005). Outliers count for the 25 per cent of the entire population. We have fitted the observed distribution with (i) an asymmetric Landau profile, peaked at 0.005 au, in the range [0.0024, 0.02 au] [defining class I (short period binary MSPs)] and (ii) a Gaussian profile, centred around 0.026 au, in the range [0.02, 0.035 au] [defining class II (long period binary MSPs)]. According to Camilo & Rasio (2005), we have assigned a companion WD mass of 0.03 $M_\odot$ for class I, and of $m_{\rm WD} = 0.2\,M_\odot$ for class II. For the binary MSPs referred to as outliers, we have taken $a_{\rm MSP,i} = 0.21$ au and $m_{\rm WD} = 0.34\,M_\odot$, corresponding to their mean properties.

5.1 Cross-sections

Table 4 collects the results obtained considering as target an IMBH of 100 $M_\odot$. We find, in the case of the single IMBH, that the cross-section is larger for the outliers compared to class I and II, due to their initially wider separation. For the [IMBH, MSP] binaries formed following the exchange of the initial stellar companion we obtain similar results, but the differences in cross-section between outliers and class I and II is less pronounced.

5.2 Orbital parameters

Fig. 6 (left-hand panel) shows the distributions of the semimajor axes of the [IMBH, MSP] binaries formed after the interactions off a single IMBH. It appears that different populations of [MSP, WD] binaries lead to the formation of [IMBH, MSP] systems with different orbital characteristics. The peak of the semimajor axis distribution for each class can be inferred from equation (7): 1.7 au for the short-period, class I binaries, 1.1 au for the long-period, class II binaries and 5.6 au for the outliers. A clear trend is also visible for the eccentricities (Fig. 7, left-hand panel): the lighter the WD is, the more eccentric (and with a narrower spread) is the orbit of the [IMBH, MSP] binary. This correlation is due to angular momentum conservation:

$$m_{\rm WD}\sqrt{\frac{{\rm G}a_{\rm MSP,i}}{m_{\rm MSP}+m_{\rm WD}}} = M_{\rm IMBH}\sqrt{\frac{{\rm G}a_{\rm MSP,f}(1-e_{\rm f}^2)}{m_{\rm MSP}+M_{\rm IMBH}}}. \quad (10)$$

Using equation (7) this implies

$$1 - e_{\rm f}^2 \propto m_{\rm WD}^3 (m_{\rm MSP}+m_{\rm WD})^{-4/3}. \quad (11)$$

Fig. 6 (right-hand panel) shows the semimajor axes of the [IMBH, MSP] systems formed after the interaction with the [IMBH, star] systems. The distributions are skewed to smaller separations,

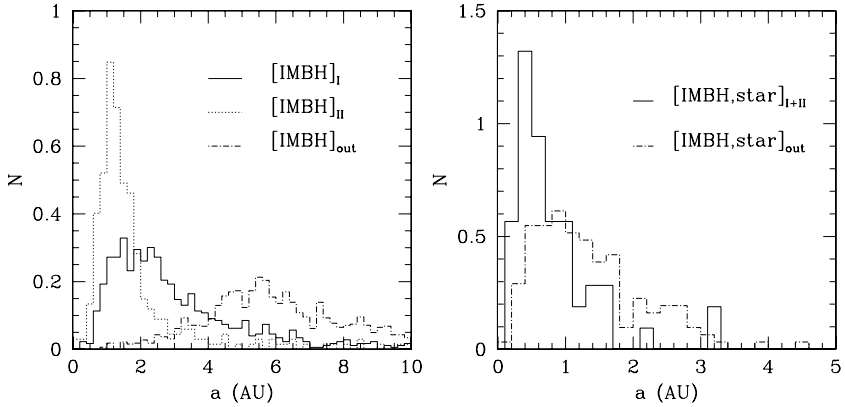

Figure 6. Distribution of the semimajor axes of [IMBH, MSP] binaries, normalized to the corresponding fraction of events. The IMBH has a mass of 100 $M_\odot$. Left-hand panel refers to encounters off the single IMBH; solid, dotted and dot–dashed lines refer to scattering with class I, class II and outliers, respectively. Right-hand panel refers to encounters off the [IMBH, star] binary: solid and dashed lines refer to 'class I and II and 'outliers, respectively.

© 2007 The Authors. Journal compilation © 2007 RAS, MNRAS **380,** 691–702

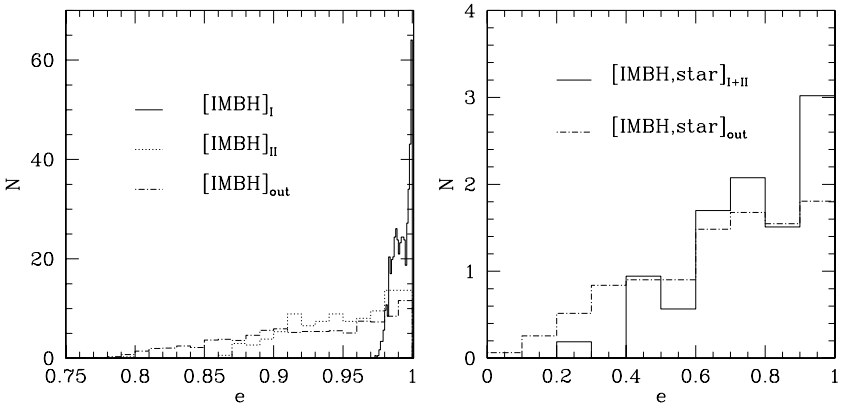

Figure 7. Distribution of the eccentricities of [IMBH, MSP] binaries, normalized to the corresponding fraction of events. The IMBH has a mass of $100\,M_\odot$. Left-hand panel refers to encounters off the single IMBH; solid, dotted and dot–dashed lines refer to scattering with class I, class II and outliers, respectively. Right-hand panel refers to encounters off the [IMBH, star] binary: solid and dashed lines refer to 'class I and II and 'outliers, respectively.

Table 3. Probability coefficient w_X as defined in Section 6, rates of formation of observable [IMBH, MSP] binaries, and lifetimes $t_{life,MSP}$, for $\langle v_* \rangle = 10$ km s^{-1}, $\langle \rho_* \rangle = 7 \times 10^5\,M_\odot\,pc^{-3}$. The channels of formation are the same as in Table 1.

$M\,(M_\odot)$	w_X	Γ_{MSP} (10^{-11} yr^{-1})	t_{life} (10^8 yr)
[100]	0.27	0.3	1.3
[300]	0.27	0.4	0.687
[100, star]	0.4	0.7	3.6
[300, star]	0.4	0.3	2.35
[100, star]$_{MSP,single}$	0.2	0.1	4.3
[300, star]$_{MSP,single}$	0.2	0.06	3.3

compared to the case of a single IMBH, due to the fact that the MSP has ejected the star (see Section 3.2). The smaller cross-section for the [IMBH, star] case compared to the single IMBH, for the family of the outliers (see Table 4), is due to the occurrence of unstable triplets where the MSP, that binds on to wider orbit (see equation 7), is preferentially expelled. Fig. 7 (right-hand panel) shows the eccentricity distribution, relative to encounters off the [IMBH, star] binaries, which turns out to be similar to that of Fig. 2.

5.3 Lifetimes

The simulations provide the semimajor axes and eccentricities of the [IMBH, MSP] systems formed. So, using equations (A2), (A3) and (A4) of Section A1, we can calculate their subsequent orbital evolution, controlled either by hardening off cluster stars or by gravitational wave back-reaction. The lifetime is defined as the sum of the time necessary for the individual binary to harden by stars until the separation a_{gw} (equation 3) is attained, plus the time for gravitational wave in-spiral at a_{gw}, that is, $t_{life} = t_h + t_{gw}$. The mean values of the binary lifetimes are reported in Table 3 for PSR-A-like initial MSP binaries, and in Table 4 for the complete population. Note that t_{life} is computed assuming that the eccentricity e_{MSP} does not vary during the hardening phase against stars. A further increase in e_{MSP} can bring the binary into the gravitational waves regime faster, while a reduction can make the binary more long-lived. The [MSP, IMBH] binaries formed are already very eccentric. If dynamical interaction tends to bring the eccentricity distribution closer to the thermal one, we then can argue that our estimated lifetimes represent lower limits.

Fig. 8 shows the characteristic lifetimes of the [IMBH, MSP] binaries described in Section 5.2. Left-hand panel refers to encounters off the single $100\,M_\odot$ IMBH. We note that the different families of [MSP, WD] binaries lead to [IMBH, MSP] systems with different lifetimes: in particular for class I, $t_{life} \approx 6 \times 10^7$ yr due to the extremely high eccentricities at which the new systems form. By contrast, class II and the outliers have higher $t_{life} \gtrsim 10^8$ yr. Right-hand panel of Fig. 8 refers to encounters of MSP binaries off the [IMBH, star] system. In this case the distributions seem not to depend strongly on the incoming binaries: outliers as well as class I and II show very similar lifetime distributions with characteristic values around 4×10^8 yr.

6 DETECTABILITY OF [IMBH, MSP] BINARIES IN GLOBULAR CLUSTERS

In Sections 3 and 5 we investigated the formation of binaries hosting an IMBH and an MSP, via single–binary and binary–binary

Table 4. Outcomes from the encounters of different kinds of binary MSPs in GCs with a single or a binary IMBH of $100\,M_\odot$. Columns: number N of runs for each set of simulations, occurrence fraction (f_{MSP} normalized to N), cross-section Σ_{MSP} (as defined in Section 3.1), probability coefficient w_X as defined in Section 6, characteristic formation rates Γ_X and lifetimes t_{life} (estimated as in Section 5.3). These times are computed considering $\langle v_* \rangle = 10$ km s^{-1}, $\langle \rho_* \rangle = 7 \times 10^5\,M_\odot\,pc^{-3}$ and a core radius of 0.75 pc. First (last) two rows refer to encounters with class I and II binaries and to outliers scattering off a single (binary) IMBH, respectively.

$M\,(M_\odot)$	N	f_{MSP} (per cent)	Σ_{MSP}(au^2)	w_X	Γ_X (10^{-11} yr)	t_{life} (10^8 yr)
[100]$_{I+II}$	10 000	10.7	260	0.2	0.2	0.6
[100]$_{outlier}$	10 000	10.8	3900	0.07	1.2	2.2
[100, star]$_{I+II}$	5000	1.8	232	0.3	0.3	4.3
[100, star]$_{outlier}$	5000	5.2	680	0.1	0.3	5.5

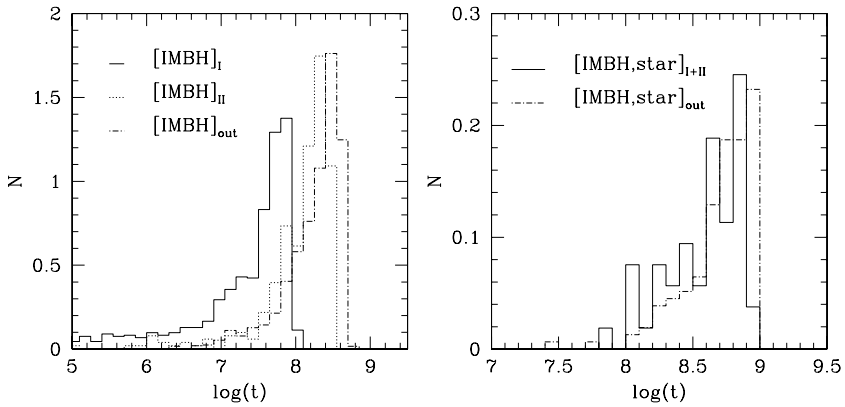

Figure 8. Distribution of the lifetimes. Lines and labels are defined as in Fig. 6.

interactions. Here, we compute their formation rates and estimate the number of expected systems in the Milky Way GCs.

The rate of formation for channel X reads

$$\Gamma_{\rm X} \sim n_{\rm MSP} w_{\rm X} \langle v_\infty \rangle \Sigma_{\rm X}, \tag{12}$$

where $n_{\rm MSP}$ is the number density of MSPs in the cluster core of radius $r_{\rm c}$, $\Sigma_{\rm X}$ the cross-section defined in equation (5) and $w_{\rm X}$ the probability coefficient (estimated below), associated to channel X.

The structural parameters of GCs span a large interval of values. In order to estimate $\Gamma_{\rm X}$, we considered only the 23 GCs that are known to host at least one MSP. For each GC in this selected sample, we computed the MSP number density as $n_{\rm MSP} \sim N_{\rm MSP}/4r_{\rm c}^3$ where $N_{\rm MSP}$ is half of the number of currently observed MSPs in every GC in order to take into account the fact that not all MSPs are hosted inside the GC's core. The mean value of $n_{\rm MSP}$ obtained considering the sample of Galactic GCs is $\approx 2 \times 10^{-14}$ au^{-3}.

For the calculation of $w_{\rm X}$, we adopted a ratio of 2 for the relative number of single and binary MSPs, in accordance with the ratio observed (Camilo & Rasio 2005). The outliers account for 25 per cent of the binary MSPs, and class I and II for 50 and 25 per cent, respectively. Following Blecha et al. (2006), we also assume that the IMBH lives as single object for ∼40 per cent of its lifetime, whereas for the remaining ∼60 per cent it is bound with a cluster star. The values of $w_{\rm X}$ are computed according to these simple recipes and are collected in Tables 3 and 4 together with the estimates mean rates $\Gamma_{\rm X}$. We note that the main contribution comes from binary MSPs belonging to the family of the outliers, scattering off the single IMBH.

As previously discussed in Section 5.3 and shown in Fig. 8, the [IMBH, MSP] binaries have characteristic lifetimes shorter than their typical formation time-scales. Consequently, the expected number of [IMBH, MSP] binaries that formed and reside in a GC is roughly given by

$$N_{\rm X} \sim t_{\rm life,X} \Gamma_{\rm X}. \tag{13}$$

We thus estimated the total number $N_{\rm tot}^{\rm exp}$ of expected [IMBH, MSP] systems (i.e. those [IMBH, MSP] in which the radio beams of the MSP sweep the direction to the Earth), summing over all channels and over the sample of GCs hosting at least one MSP. We find $N_{\rm tot}^{\rm exp} \sim 0.1$, if a $\sim 100\,{\rm M}_\odot$ IMBH is hosted in *all* the GCs which are currently known to include an MSP. Thus, the detection of an [IMBH, MSP] binary has at present a low probability of occurrence.[5]

The derived value of $N_{\rm tot}^{\rm exp}$ is a firm lower limit since $n_{\rm MSP}$ represents a lower limit to the MSP density in a GC core, given that we considered only the already detected MSPs. The ongoing deep surveys running at GBT (Ransom et al. 2005), GMRT (Freire et al. 2004) and Parkes (Possenti et al. 2003) are rapidly increasing the known population of MSPs in GCs, suggesting that additional clusters may contain a rich population of MSPs. The likelihood of unveiling a binary [IMBH, MSP] will become significantly higher when new more powerful radio telescopes will become available. In particular the planned Square Kilometre Array (SKA; Cordes et al. 2004) is expected to improve by one to two orders of magnitude the sensitivity limits of the present instruments. That will allow us to probe the faintest end of the luminosity function of the MSPs in GCs. If the current extrapolations of this luminosity function (Camilo & Rasio 2005; Ransom et al. 2005) will turn out to be correct, an order of magnitude more MSPs could be found in the core of the Galactic GCs, that have been missed by the current surveys due to their relative faintness. In this case, $N_{\rm tot}^{\rm exp} \approx 1$ and SKA will be able to detect all of this kind of systems. Therefore, a complete search for MSPs in the GCs of the Milky Way with SKA will have the potentiality of testing the hypothesis that IMBHs of the order of $100\,{\rm M}_\odot$ are commonly hosted in GCs.

The detection of one [IMBH, MSP] system will immediately give the chance of measuring the mass of the IMBH from pulsar timing with at least 1 per cent accuracy (Cordes et al. 2004). Even more interesting, the presence of a very stable clock (like MSPs usually are) orbiting a probably rotating $\sim 100\,{\rm M}_\odot$ BH makes this system a potentially unique laboratory of relativistic physics. In fact, many still elusive higher order relativistic effects depend on the spin and on the quadrupole moment of the rotating BH (Wex & Kopeikin 1999) and the latter two quantities scale with the mass squared and the mass cubed of the BH, respectively. Therefore, an [IMBH, MSP] binary is a more promising target for studying the physics in the surroundings of a BH (Kramer et al. 2004) than a binary comprising an MSP and a stellar mass BH.

[5] No strong bias against the detection of an [IMBH, MSP] binary is caused by its the orbital motion. In fact, Patruno et al. (2005) showed that the discovery of a bright MSPs orbiting an IMBHs at mean separations of a few au is not hampered by the Doppler modulation of the radio pulses.

7 SUMMARY

In this paper, we investigated the dynamical processes leading to the capture of an MSP by an IMBH in the dense core of a GC. We simulated single–binary and binary–binary encounters between an IMBH and an MSP, either single or with a WD companion. The binary MSPs have masses and orbital parameters chosen according to the distribution observed in a sample of 23 GCs. In order to account for all the possible configurations of IMBHs hosted in GCs, we have considered the case of a single IMBH, of an [IMBH, star] binary and of an [IMBH, BH] binary. For each of these cases we derived the cross-section for the formation of [IMBH, MSP] and [IMBH, WD] binaries, as well as the distribution of the final semimajor axes and eccentricities of such newly formed binaries.

The main outcomes from this study are as follows.

(i) Dynamical encounters of an MSP with either single IMBHs or [IMBH, star] binaries promote the formation of [IMBH, MSP] binaries in $\sim$10 and $\sim$1$-$5 per cent of the calculated interactions, respectively. Similar rates were found for the formation of [IMBH, WD] binaries. The final distributions of semimajor axes and eccentricities of the formed [IMBH, MSP] and [IMBH, WD] binaries are found to be in agreement with previous semi-analytical models (Pfahl 2005).

(ii) We found that the presence of a stellar mass BH, orbiting around the IMBH, strongly inhibits the formation of an [IMBH, MSP] binary. Only in a small minority of cases ($\sim$0.2 per cent), interactions between an [IMBH, BH] binary and an MSP can allow for the formation of a stable hierarchical triple, where the MSP occupies the external orbit. When the internal [IMBH, BH] binary merges due to orbital decay by gravitational waves emission, the triple evolves into a new [IMBH, MSP] binary.

(iii) The [IMBH, MSP] binaries are expected to form with very high eccentricities ($e \sim 0.9$) and tight orbits ($\lesssim$7 au). This means that they can be important sources of gravitational waves, either in the in-spiral phase or in the final merging event.

(iv) Due to the aforementioned gravitational quadrupole radiation, the [IMBH, MSP] binaries are relatively short-lived, inspiralling to coalescence in $\sim 10^8$ yr. This lifetime is significantly shorter than the estimated formation time-scale of [IMBH, MSP] binaries which may be detectable with the present instrumentation.

(v) If IMBHs of $\sim 100\,M_\odot$ are commonly hosted in the Galactic GCs, next-generation radio telescopes, like SKA, will have the possibility of detecting at least one of these exotic binaries.

ACKNOWLEDGMENTS

We thank S. Aarseth for enlightening discussions and for having kindly provided us the code CHAIN. We thank the Referee for her/his critical comments that allowed us to significantly improve the manuscript. MC and AP acknowledge financial support from MURST, under the grant PRIN-2005024090.

REFERENCES

Baumgardt H., Makino J., McMillan S., Portegies Zwart S., 2003a, ApJ, 582, L21
Baumgardt H., Makino J., McMillan S., Portegies Zwart S., 2003b, ApJ, 589, L25
Baumgardt H., Makino J., Ebisuzaki T., 2004, ApJ, 613, 1143
Bassa C. G., Verbunt F., van Kerkwijk M. H., Homer L., 2003, A&A, 409, L31
Blecha L., Ivanova N., Kalogera V., Belczynski K., Fregeau J., Rasio F. A., 2006, ApJ, 642, 427
Camilo F., Rasio F. A., 2005, in Rasio F. A., Stairs I. H., eds, ASP Conf. Ser. Vol. 328, Binary Radio Pulsars. Astron. Soc. Pac., San Francisco, p. 147
Colpi M., Possenti A., Gualandris A., 2002, ApJ, 570, L85
Colpi M., Mapelli M., Possenti A., 2003, ApJ, 559, 1260
Cordes J. M., Kramer M., Lazio T. J. W., Stappers B. W., Backer D. C., Johnston S., 2004, New Astron. Rev., 48, 1413
Corongiu A., Possenti A., Lyne A. G., Manchester R. N., Camilo F., D'Amico N., Sarkissian J. M., 2006, ApJ, 653, 1417
D'Amico N., Possenti A., Fici L., Manchester R. N., Lyne A. G., Camilo F., Sarkissian J., 2002, ApJ, 570, L89
Dubath P., Meylan G., Mayor M., 1997, A&A, 324, 505
Ferrarese L., Merritt D., 2000, ApJ, 539, L9
Ferraro F. R., Possenti A., Sabbi E., Lagani P., Rood R. T., DÁmico N., Origlia L., 2003a, ApJ, 595, 179
Ferraro F. R., Possenti A., Sabbi E., DÁmico N., 2003b, ApJ, 596, L211
Freire P. C., Gupta Y., Ransom S. M., Ishwara-Chandra C. H., 2004, ApJ, 606, L53
Freitag M., Gürkan M. A., Rasio F. A., 2006, MNRAS, 368, 141
Gebhardt K. et al., 2000, ApJ, 539, L13
Gebhardt K., Rich R., Ho L. C., 2002, ApJ, 578, L41
Gebhardt K., Rich R., Ho L. C., 2005, ApJ, 634, 1093
Gerssen J., van der Marel R. P., Gebhardt K., Guhathakurta P., Peterson R. C., Pryor C., 2002, AJ, 124, 3270
Gürkan M. A., Fregeau J. M., Rasio F. A., 2006, ApJ, 640, L39
Harris W. E., 1996, AJ, 112, 1487 (Updated version at http://www.physics.mcmaster.ca/resources/globular.html)
Hills J. G., 1975, AJ, 80, 1075
Hut P., Bahcall J. N., 1983, ApJ, 268, 319
Khalisi E., Amaro-Seoane P., Spurzem R., 2007, MNRAS, 374, 703
Kramer M., Backer D. C., Cordes J. M., Lazio T. J. W., Stappers B. W., Johnston S., 2004, New Astron. Rev., 48, 993
Kulkarni S. R., Hut P., McMillan S., 1993, Nat, 364, 421
Lightman A. P., Fall S. M., 1978, ApJ, 221, 567
McLaughlin D. E., Anderson J., Meylan G., Gebhardt K., Pryor C., Minniti D., Phinney S., 2006, ApJ, 166, 249
Maccarone T. J., Kundu A., Zepf S. E., Rhode K. L., 2007, Nat, 445, 183
Mapelli M., Colpi M., Possenti A., Sigurdsson S., 2005, MNRAS, 364, 1315
Mardling R., Aarseth S., 1999, in Steves B. A., Roy A. E., eds, NASO ASI Ser. C, Vol. 522, The Dynamics of Small Bodies in the Solar System. Kluwer, Boston, p. 385
Miller M. C., Hamilton D. P., 2002, MNRAS, 330, 232
Monkman E., Sills A., Howell J., Guhathakurta P., de Angeli F., Beccari G., 2006, ApJ, 650, 195
O'Leary M. J., Ryan M., Rasio F. A., Fregeau J. M., Ivanova N., O'Shaughnessy R., 2006, ApJ, 637, 937
Orosz J. A., 2003, in van der Hucht K., Herrero A., Esteban C., eds, Proc. IAU Symp. 212, A Massive Star Odyssey: From Main Sequence to Supernova. Astron. Soc. Pac., San Francisco, p. 365
Patruno A., Colpi M., Faulkner A., Possenti A., 2005, MNRAS, 364, 344
Peters P. C., Mathews J., 1963, Phys. Rev., 131, 435
Pfahl E., 2005, ApJ, 626, 849
Portegies Zwart S. F., McMillan S. L. W., 2000, ApJ, 528, L17
Portegies Zwart S. F., McMillan S. L. W., 2002, ApJ, 576, 899
Possenti A., D'Amico N., Manchester R. N., Camilo F., Lyne A. G., Sarkissian J., Corongiu A., 2003, ApJ, 599, 475
Quinlan G. D., 1996, New Astron., 1, 255
Ransom S. M., Hessels J. W. T., Stairs I. H., Freire P. C. C., Camilo F., Kaspi V. M., Kaplan D. L., 2005, Sci, 307, 892
Sigurdsson S., 2003, in Bailes M., Nice D. J., Thorsett S. E., eds, ASP Conf. Ser. Vol. 3, Radio Pulsars. Astron. Soc. Pac., San Francisco, p. 391
Sigurdsson S., Hernquist L., 1993, Nat, 362, 423
Sigurdsson S., Phinney E. S., 1993, ApJ, 415, 631
Spitzer L., 1969, ApJ, 158, 161
Suzuki T. K., Nakasato N., Baumgardt H., Ibukiyama A., Makino J., Ebisuzaki T., 2007, ApJ, submitted (astro-ph/0703290)

van den Bosch R., de Zeeuw T., Gebhardt K., Noyola E., van de Ven G., 2006, ApJ, 641, 852
Watters W. A., Joshi K. J., Rasio F. A., 2000, ApJ, 539, 331
Wex N., Kopeikin S., 1999, ApJ, 513, 338

APPENDIX A: INITIAL CONDITIONS

A1 Initial semimajor axis distribution

We describe here in some detail how we generate the initial distribution for the semimajor axis of the IMBH binaries.

(i) IMBH, star: We have followed the analysis of Pfahl (2005) who considers the tidal disruption of a stellar binary off an IMBH. From considerations on energy conservation, the semimajor axes a_* of the newly formed binary follows the relation

$$a_* = \frac{1}{2} a_{\rm b} \frac{m_{\rm b}}{m_{\rm esc}} \left(\frac{M_{\rm IMBH}}{m_{\rm b}} \right)^{2/3}, \tag{A1}$$

where $m_{\rm b}$ is the mass of the initial binary, $a_{\rm b}$ its semimajor axis and $m_{\rm esc}$ the mass of the escaping star (see also the discussion in Section 3.2). To reproduce the initial distribution for a_*, we have considered a uniform distribution for the mass ratio of the stellar binary $q \equiv m_1/m_2$ and a distribution homogeneous in $\log(a_b)$ for the values of the semimajor axes of the incoming binary in the range [0.01, 10 au]. The upper and lower limits obtained are reported in Table 1. Fig. A1 shows the initial distributions of a_* (left-hand panel) and e_* (right-hand panel). Note that the distribution of a_* is harder than that found in Blecha et al. (2006).[6] If the real distribution would be less hard as in Blecha et al. (2006), our resulting [IMBH, MSP] formation rates for the [IMBH, star] case should be considered as a lower limit. Indeed a less bound initial companion to the IMBH would be more easily ejected by the unstable triple interaction with the MSP (see Section 3.2).

(ii) IMBH, BH: We expect that [IMBH, BH] binaries can form dynamically in the core of a GC. If the IMBH has been formed through a succession of gravitational encounters with stellar mass BHs, then we expect some of these to be ejected in the outer region of the GC and to sink back to the core by dynamical friction (Sigurdsson & Hernquist 1993). The formation of the [IMBH, BH] binary can then be the result of one of the following interactions:

IMBH+[BH, star] $\rightarrow$ [IMBH, BH] + star;

[IMBH, star] + [BH, star] $\rightarrow$ [IMBH, BH] + stars;

[IMBH, star] + BH $\rightarrow$ [IMBH, BH] + star.

The [IMBH, BH] binary just formed is assumed to have a separation comparable to the IMBH influence radius. This is not our initial condition for simulating the encounters with the [MSP, WD] systems, since we have accounted for the intrinsic long-term evolution of the [IMBH, BH] binary parameters. Accordingly, we have generated the values of the initial [IMBH, BH] binary semimajor axis (i.e. the values of $a_{\rm BH}$ from which we start the three- or four-body simulations) from a distribution obtained sampling uniformly in time when considering the evolution of $a_{\rm BH}$ due to the hardening (i) off cluster stars and (ii) by gravitational wave back-reaction.

In phase (i), denoted in the text as $[\mathrm{IMBH, BH}]_{\rm h,*}$, the evolution of $a_{\rm BH}$ is governed by the equation

$$\frac{{\rm d}a_{\rm BH}}{{\rm d}t} = -(2\pi\xi)\,\frac{G\langle\rho_*\rangle}{\langle v_*\rangle} a_{\rm BH}^2, \tag{A2}$$

holding until $a_{\rm BH} = a_{\rm gw}(e_{\rm BH} = 0.7)$ set by equation (3) (Hills 1975). In equation (A2) we assumed fixed the values of $\langle\rho_*\rangle = 7 \times 10^5\,{\rm M}_\odot\ {\rm pc}^{-3}$ and $\langle v_*\rangle = 10\,{\rm km\ s}^{-1}$ inferred averaging over the current GC sample described in Section 6. A change in $\langle\rho_*\rangle$ and $\langle v_*\rangle$ due to the internal evolution of the GC should also change the $a_{\rm BH}$ distribution. In particular, a lower value for the stellar density should enhance the right-hand tail of the distribution. We argue that in this case the formation of [IMBH, MSP] binaries could be enhanced. Indeed, the presence of an initial companion, bound to the IMBH on a less tight orbit than that considered in our study, would be more easily ejected by the MSP (see Section 3.2).

In phase (ii), the binary hardens by gravitational waves back-reaction (phase denoted with $[\mathrm{IMBH, BH}]_{\rm gw}$). The evolution of the orbital parameters are given by (Peters & Mathews 1963)

$$\frac{{\rm d}a_{\rm BH}}{{\rm d}t} = -\frac{64}{5}\frac{G^3 m_{\rm BH} M_{\rm IMBH}\,(m_{\rm BH} + M_{\rm IMBH})}{c^5 a_{\rm BH}^3} f(e_{\rm BH}), \tag{A3}$$

$$\frac{{\rm d}e_{\rm BH}}{{\rm d}t} = -\frac{304}{15}\frac{G^3 m_{\rm BH} M_{\rm IMBH}\,(m_{\rm BH} + M_{\rm IMBH})}{c^5 a_{\rm BH}^4} g(e_{\rm BH}), \tag{A4}$$

where

$$f(e_{\rm BH}) = \left(1 - e_{\rm BH}^2\right)^{-7/2} \left(1 + \frac{73}{24} e_{\rm BH}^2 + \frac{37}{96} e_{\rm BH}^4\right), \tag{A5}$$

$$g(e_{\rm BH}) = \left(1 - e_{\rm BH}^2\right)^{-5/2} e_{\rm BH} \left(1 + \frac{121}{304} e_{\rm BH}^2\right). \tag{A6}$$

The above equations (A3)–(A6) are integrated with the initial condition: $a_{\rm BH} = a_{\rm gw}(e_{\rm BH})$ and a trial distribution for $e_{\rm BH}$ that follows the thermal distribution. Fig. A2 shows the resulting distribution for $a_{\rm BH}$ and $e_{\rm BH}$ during the two different regimes.[7]

A2 The integration

In this subsection we describe details on the integration of three- and four-body encounters with the codes CHAIN and FEBO. For each run we divide the integration into two parts. (1) We consider the two binaries as point-like objects until their centres of mass are at a distance larger than 50 times the semimajor axis of the IMBH binary. (2) When this critical distance is reached, we start the four-body integration. As a consequence, the time spent in the two-body approximation decreases as the semimajor axes of the IMBH binary become wider. Correspondingly, the overall integration time gets longer the wider the semimajor axis of the IMBH binary is, and it becomes prohibitively long for large values of $a_{\rm BH}$ (or a_* for the [IMBH, star] binaries). For this reason, we insert a cut-off at 5 au. For wider systems, we expect that the available binding energy of the IMBH binary is insufficient to unbind the [MSP, WD] binary, so that the ionization of the binary can be mainly due to the tidal effect of the massive IMBH.

[6] We note that in their simulation, Blecha et al. (2006) consider stellar cluster considerably different from ours. Indeed, they study the formation of [IMBH, star] binaries in young clusters (their simulation stops after 100 Myr) with a correspondingly different population of stellar binaries. We argue that this can be the main cause of the difference in the distribution of a_*.

[7] Note that in phase (ii), the distribution should not be affected by any change in the structural parameters of the GC, depending only on the orbital parameters (see equations A3 and A4).

© 2007 The Authors. Journal compilation © 2007 RAS, MNRAS **380,** 691–702

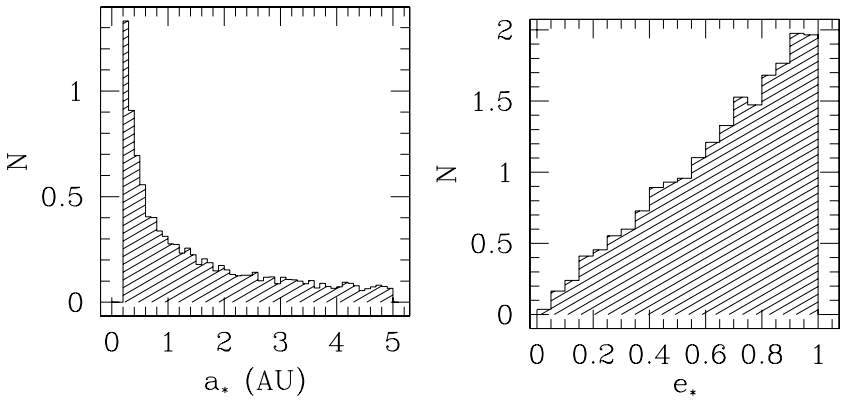

Figure A1. Initial distribution of the semimajor axes (left-hand panel) and eccentricities (right-hand panel) of the initial states [IMBH, star] for the $M_{\rm IMBH} = 100\,{\rm M}_{\odot}$.

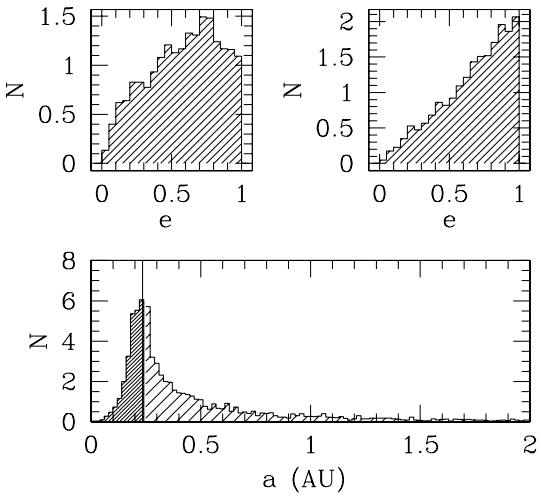

Figure A2. Upper panels: The distribution for the initial eccentricity of the [IMBH, BH] binaries are shown in the regimes of hardening-off stars (right-hand panel) and gravitational waves (left-hand panel), for $M_{\rm IMBH} = 100\,{\rm M}_{\odot}$. Lower panel: The distributions of the initial semimajor axes for the same systems are shown. The solid vertical line separates the gravitational wave regime (left-hand side) and the hardening-off stars regime (right-hand side).

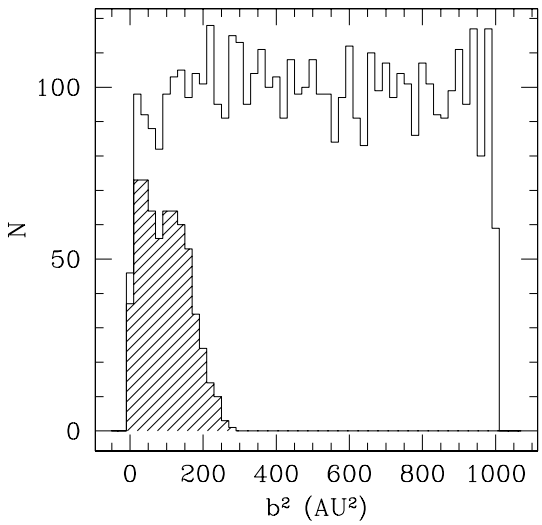

Figure A3. Distribution of impact parameters giving rise to the formation of an [IMBH, MSP] system (hatched histogram), compared to the initial (empty histogram) for the case of encounters of PSR-A like [MSP, WD] binaries off the single $100\,{\rm M}_{\odot}$ IMBH. The hatched distribution drops to zero at 300 au^2, while $b^2_{\rm max} = 1000$ au^2.

A3 Impact parameters

In this subsection we focus out attention on the choice of the maximum impact parameter $b_{\rm max}$ for a correct determination of the cross-section. According to gravitational focusing, a point mass with impact parameter b, moving at infinity with relative velocity v_{∞}, has pericentre

$$p \sim \frac{b^2\, v_{\infty}^2}{2GM_{\rm IMBH}}. \qquad \text{(A7)}$$

For the single IMBH, the maximum value of the periastron $p_{\rm max}$ is set at a few tidal radii $r_{\rm T}$; while for a binary IMBH, the value of the maximum impact parameter for a non-negligible energy exchange is typically limited up to a value of the order of a few semimajor axis of the binary IMBH, that is, $p_{\rm max} \sim x a_{\rm BH}$ or $p_{\rm max} \sim x a_{*}$ (Hills 1975), where x is close to 3 in all cases. In each run $b^2_{\rm max}$ is assigned using equation (A7). In order to guarantee that we have accounted for all the impact parameters leading to the formation of an [IMBH, MSP] (or [IMBH, WD]) binary, and to guarantee cross-section convergence, we verified a posteriori that the distribution of all relevant b^2 leading to the desired end states, drops to zero well before $b^2_{\rm max}$. Fig. A3 illustrates the case of the single $100\,{\rm M}_{\odot}$ IMBH interacting with the PSR-A like [MSP, WD] binary. The encounters ending with the formation of [IMBH, MSP] binaries are the ones represented in the hatched area. Clearly, the distribution drops to zero well before $b^2_{\rm max}$.

In the channels where either the tidal radius of the incoming binary MSP, or the semimajor axis of the IMBH binary vary from encounter to encounter (according to the initial distributions described in Section 2.2 for the binary IMBH, and in Section 5 for the binary MSP), we allowed $b^2_{\rm max}$ to vary accordingly, and defined a mean $\langle b^2_{\rm max}\rangle$, obtained averaging over all choices of $r_{\rm T}$ and/or a_{*} ($a_{\rm BH}$). This average is used to compute the cross-section in equation (5).

This paper has been typeset from a TEX/LATEX file prepared by the author.